



# Manganese dioxide as a new cathode catalyst in microbial fuel cells

Xiang Li<sup>a</sup>, Boxun Hu<sup>b</sup>, Steven Suib<sup>b,c,d</sup>, Yu Lei<sup>d</sup>, Baikun Li<sup>a,\*</sup>

<sup>a</sup> Department of Civil and Environmental Engineering, University of Connecticut, Storrs, CT 06269, United States

<sup>b</sup> Institute of Materials Science, University of Connecticut, Storrs, CT 06269, United States

<sup>c</sup> Department of Chemistry, University of Connecticut, Storrs, CT 06269, United States

<sup>d</sup> Department of Chemical and Biomolecular Engineering, University of Connecticut, Storrs, CT 06269, United States

## ARTICLE INFO

### Article history:

Received 23 September 2009

Received in revised form 28 October 2009

Accepted 29 October 2009

Available online 14 November 2009

### Keywords:

Microbial fuel cells

Manganese dioxides

Octahedral molecular sieves

Oxygen reduction reaction

## ABSTRACT

This study focused on manganese oxides with a cryptomelane-type octahedral molecular sieve (OMS-2) structure to replace platinum as a cathode catalyst in microbial fuel cells (MFCs). Undoped (ud-OSM-2) and three catalysts doped with cobalt (Co-OMS-2), copper (Cu-OMS-2), and cerium (Ce-OMS-2) to enhance their catalytic performances were investigated. The novel OMS-2 cathodes were examined in granular activated carbon MFC (GACMFC) with sodium acetate as the anode reagent and oxygen in air as the cathode reagent. The results showed that after 400 h of operation, the Co-OMS-2 and Cu-OMS-2 exhibited good catalytic performance in an oxygen reduction reaction (ORR). The voltage of the Co-OMS-2 GACMFC was 217 mV, and the power density was 180 mW m<sup>-2</sup>. The voltage of the Cu-OMS-2 GACMFC was 214 mV and the power density was 165 mW m<sup>-2</sup>. The internal resistance ( $R_{in}$ ) of the OMS-2 GACMFCs ( $18 \pm 1 \Omega$ ) was similar to that of the platinum GACMFCs ( $17 \Omega$ ). Furthermore, the degradation rates of organic substrates in the OMS-2 GACMFCs were twice those in the platinum GACMFCs, which enhance their wastewater treatment efficiencies. This study indicated that using OMS-2 manganese oxides to replace platinum as a cathodic catalyst enhances power generation, increases contaminant removal, and substantially reduces the cost of MFCs.

Published by Elsevier B.V.

## 1. Introduction

Microbial fuel cell (MFC) technology is an emerging biotechnology that utilizes bacteria to generate electricity from the degradation of organic substances [1]. Traditional MFCs consist of an anaerobic anode and an aerobic cathode. Bacteria degrade organic substances (e.g., acetate, glucose) and generate electrons in the anode chamber. The electrons are transferred to the anode surfaces, which then flow through an external circuit to react with an electron acceptor (e.g., oxygen, ferricyanide) in the cathode chamber, through which electricity is produced. MFCs can efficiently convert organic contaminants to clean energy at normal temperatures and pressures, which holds great potential for their application in wastewater treatment plants to simultaneously treat wastewater and produce energy.

A large effort has been invested to enhance energy production in MFCs. Most attention was on substrate degradation, electron generation, and transfer in anode chambers [2]. Several important factors including substrate concentration, pH, conductivity, microbial activity, circuit resistance, electrode, and membrane material have been extensively investigated [3,4]. However, in recent stud-

ies, oxygen reduction and electron acceptance in the cathode chamber have been found as the limiting step for energy production due to the slow reaction kinetics of the oxygen reduction rate (ORR) [5,6]. Platinum (Pt) has been widely used as the cathode catalyst to accelerate the ORR and electron acceptance in MFCs [7], but the high cost of platinum poses an obstacle in the application of MFCs. Low cost non-Pt catalysts are needed to reduce the cost of MFCs. Iron (II) and cobalt-based cathodes were reported to show similar performances as platinum. But long-term stability of these materials is not satisfied [8,9].

In the past decade, manganese dioxide has been studied as a promising alternative to platinum in methanol and borohydride fuel cells [10,11]. Catalysts with a cryptomelane-type octahedral molecular sieve (OMS-2) structure have been of interest as cathode catalysts due to their excellent semi-conductivity and catalytic activity in ORRs. There are only a few studies of applying manganese oxide in MFCs. Zhang et al. reported that  $\beta$ -MnO<sub>2</sub> is the most effective catalyst among the three OMS structures ( $\alpha$ ,  $\beta$ , and  $\gamma$ -MnO<sub>2</sub>) due to its highest Brunauer–Emmett–Teller (BET) surface area and average oxidation state (AOS: 3.6) of manganese [12]. Roche et al. employed the manganese oxide as the cathode catalyst, and obtained the peak power density of 161 mW m<sup>-2</sup>. They also found that the performances of manganese oxide catalysts were easily improved by optimizing operation conditions [13]. Suib et al. reported that the tuning of AOS by the incorporation of dif-

\* Corresponding author. Tel.: +1 860 486 2339; fax: +1 860 486 2298.

E-mail address: [baikun@engr.uconn.edu](mailto:baikun@engr.uconn.edu) (B. Li).

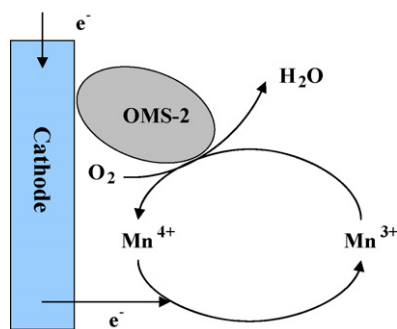
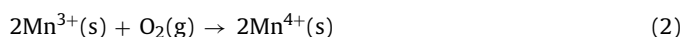
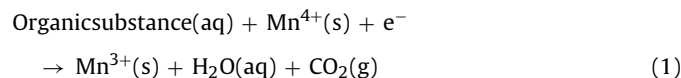


Fig. 1. The possible mechanism for oxygen reduction rate (ORR) with OMS-2 catalysts.

ferent transitional metal ions to obtain an AOS of 3.9–4.0 could generate the highest reaction rate and catalytic activity [14]. Synthetic OMS-2 showed outstanding electrochemical and catalytic properties among the  $\text{MnO}_2$  group; electrons could easily flow in particular OMS-2 materials; and doping of these materials created differences of orders of magnitude in conductivity [15].

Previous research on the oxidation mechanism of organic substances with OMS-2 shows that kinetic data fit the Mars-van Krevelen (MvK) model of heterogeneously catalyzed reactions [16]. In a typical MFC, oxygen passes through a polytetrafluoroethylene (PTFE) diffusion layer and is adsorbed on OMS-2 catalysts (Fig. 1). Organic substances are adsorbed and bound to the oxygen vacancies of OMS-2 catalysts. A redox mechanism is considered to involve carbohydrate oxidation by  $\text{Mn}^{4+}\text{O}_2^-$ , which is reduced to  $\text{Mn}^{3+}$  Reaction (1).  $\text{Mn}^{3+}$  ions are reoxidized by dioxygen Reaction (2).  $\text{Mn}^{4+}$  is an electron acceptor and the formation of dioxygen manganese complexes leads to production of oxygen which could be used in the cathodic reaction.



Compared with platinum, manganese oxide featuring the OMS-2 structure has the following advantages: (i) there is a fast oxygen reduction rate and conductivity ( $0.53 \Omega^{-1} \text{cm}^{-1}$ ); (ii) there is a much higher specific surface area ( $50 \text{m}^2 \text{g}^{-1}$ ) than the platinum coated carbon cloth ( $18 \text{m}^2 \text{g}^{-1}$ ); (iii) manganese oxide is less expensive than Pt catalysts; the price of a Pt catalyst is 20 times that of a manganese catalyst. Therefore, the objective of this study was to investigate the feasibility of using  $\text{MnO}_2$  as cathode catalysts in MFCs to enhance power generation and substrate degradation. The undoped OMS-2 and three doped OMS-2 catalysts were examined in terms of electrochemical and biochemical reactions in MFCs. The performance of OMS-2 catalysts was also compared with that of platinum to explore the possibility of using OMS-2 to replace platinum as cost-effective cathode catalysts in MFCs.

## 2. Materials and methods

### 2.1. Catalyst preparation

The OMS-2 cathode catalysts were synthesized using hydrothermal methods. The synthesized paper-like OMS-2 membrane cathode is a better conductor than the bulk OMS-2 powder cathode due to the alignment and connectivity of the microporous network in the membrane. The synthesis of an undoped (ud)-OMS-2 membrane was described in a previous study [17], in which a 32 mmol mixture of  $\text{K}_2\text{S}_2\text{O}_8$ ,  $\text{MnSO}_4$ ,  $\text{K}_2\text{SO}_4$  (molar ratio: 3:2:3) was dis-

solved in 70 mL deionized water for the hydrothermal synthesis. Three typical dopings (cobalt  $\text{Co}^{3+}$ , copper  $\text{Cu}^{2+}$ , and cerium  $\text{Ce}^{4+}$ ) that have been previously examined and found to exhibit high catalyst performances were selected in this study [18]. In the synthesis of Co-OMS-2 catalyst, 28 mmol of  $\text{Co}(\text{OH})_3$ ,  $\text{MnSO}_4$ ,  $\text{K}_2\text{SO}_4$  (molar ratio: 2:2:3) was mixed with 70 mL  $\text{H}_2\text{O}$  in a 125 mL autoclave. The autoclave was sealed in a stainless steel Parr bomb and then heated in an oven at  $180^\circ\text{C}$  for 48 hr. The slurry was washed with 1 L deionized (DI) water and dried in an oven at  $100^\circ\text{C}$  for 12 h. The syntheses of Ce-OMS-2 and Cu-OMS-2 followed the same procedures but used different recipes. The Ce-OMS-2 preparation used 28 mmol of  $\text{Ce}(\text{SO}_4)_2$ ,  $\text{MnSO}_4$ ,  $\text{K}_2\text{SO}_4$  (molar ratio: 2:2:3) and 70 mL  $\text{H}_2\text{O}$ . The Cu-OMS-2 preparation used 30 mmol of  $\text{CuSO}_4$ ,  $\text{K}_2\text{S}_2\text{O}_8$ ,  $\text{MnSO}_4$ ,  $\text{K}_2\text{SO}_4$  (molar ratio: 1:20:20:30), and 70 mL  $\text{H}_2\text{O}$ . The OMS-2 catalyst loading on cathodes was  $0.5 \text{mg cm}^{-2}$  in all tests.

Platinum was used as the control for the cathode catalysts. The platinum cathode was made following the method used in a previous study [7], in which  $0.5 \text{mg cm}^{-2}$  Pt catalysts were bonded on a carbon cloth using a Nafion solution (Aldrich, St. Louis, MO).

### 2.2. Electrode preparation

A typical OMS-2 cathode is composed of four layers in this sequence: a PTFE diffusion layer, a carbon powder layer, a carbon cloth layer, and an OMS-2 catalyst layer. In the preparation of the OMS-2 cathode, a carbon powder layer composed of 64.0 mg of ground carbon black powder (Cabot Vulcan XC-72) and 3.2 mL 30% PTFE solution (Aldrich, St. Louis, MO) was coated on a carbon cloth ( $8 \text{cm} \times 8 \text{cm}$ ). A PTFE layer was then coated on the carbon powder layer with a 60% PTFE suspension using a paintbrush. After each coating layer was finished, the cathode was air-dried for 4 h and then was dried in an oven at  $370^\circ\text{C}$  for 20 min. Next, a pulp-like mixture of 160 mg OMS-2 powder, 4.5 mL water, and 2.1 mL Nafion solution (Aldrich, St. Louis, MO) was spin-coated on the opposite side of the PTFE diffusion layer on the carbon cloth. Finally, this OMS-2 coated cathode was air-dried overnight in a hood.

### 2.3. MFC set-up and operation

Granular activated carbon single-chamber microbial fuel cells (GACMFCs) used in this study were described previously [19]. The volume of the GACMFC was 0.6 L. About 230 g of GAC particles (GC  $8 \times 30$ , General Carbon, Paterson, NJ) was packed into the MFC and used as the anode. The catalyst coated carbon cloth was screwed on top of the MFC and used as the cathode. Influent collected at the University of Connecticut wastewater treatment plant was used as the inoculum. The initial chemical oxygen demand (COD) of wastewater was about  $200 \text{mg L}^{-1}$ , the pH was 7.2, and the dissolved oxygen was  $3.0 \text{mg L}^{-1}$ . Supplemental sodium acetate was added to domestic wastewater to achieve the designated COD concentrations for the GACMFC tests. The external resistance ( $R_{\text{ext}}$ ) was  $100 \Omega$  unless otherwise stated. The voltage over  $R_{\text{ext}}$  was recorded by a Keithley 2700 data logging system at 2 h intervals. All experiments were conducted in a  $30^\circ\text{C}$  incubator.

### 2.4. Electrochemical measurement

The internal resistance ( $R_{\text{in}}$ ) is the resistance existing within the MFCs. This resistance consumes the power generated by the MFCs and lowers the power generation efficiency. The  $R_{\text{in}}$  was determined by electrochemical impedance spectroscopy (EIS) using a potentiostat.

The open circuit potentials (OCP) of anodes and cathodes in MFCs were measured using a potentiostat (Gamry Reference 600), with the target electrode (anode or cathode) as the working pole,

and an Ag/AgCl reference electrode as the counter pole and the reference pole.

Electrochemical analysis of OMS-2 was also carried out by the linear sweep voltammetry (LSV). Measurements were performed using a CHI 601C electrochemical workstation (CH Instruments, USA). All experiments were conducted using a three-electrode electrochemical cell, with a working electrode, an Ag/AgCl reference electrode and a platinum counter electrode. LSV was taken from  $-0.6$  V to  $0$  V in  $1$  M phosphate buffer solution (PBS, pH =  $7.0$ ) with a scan rate of  $250$  mV s $^{-1}$ .

Power densities (W m $^{-2}$ ) and (A m $^{-2}$ ) were calculated from the cell voltage  $V$  (V), external resistor  $R_{\text{ext}}$  ( $\Omega$ ), and area of the cathode  $A$  (m $^2$ ) according to power density =  $V^2/R_{\text{ext}}A$  and current density =  $V/R_{\text{ext}}A$ . The external resistors ( $R_{\text{ext}}$ ) were changed from  $46$  to  $1500$   $\Omega$  during the polarization curve measurement, and the voltage over each  $R_{\text{ext}}$  was recorded by a multimeter.

Coulombic efficiency (CE,  $\eta_c$  %) was defined as the ratio of the actual charge generated to the theoretical charge generated if the substrate is completely converted to electricity. The CE was calculated based on the equation previously reported [2].

### 2.5. Scanning electron microscopy (SEM) observation of the cathodes

The morphology of cathodes was observed using an SEM (Model: Joel6335F). The cathodes were fixed for  $12$  h at  $4^\circ\text{C}$  in a mixed solution containing  $2.5\%$  paraformaldehyde,  $1.5\%$  glutaraldehyde and  $0.1$  M cocadylate buffer (pH  $7.4$ ) before being washed three times with cocadylate buffer. The samples were dehydrated in a series of ethanol/water solution (the volume ratios of ethanol-to-water:  $25\%$ ,  $50\%$ ,  $70\%$ ,  $85\%$ ,  $95\%$ , and  $100\%$ ) for  $15$  min [7]. The sample was then completely dried in an anaerobic environment at  $30^\circ\text{C}$  and sputtered with gold at  $2.2$  kV,  $10$  mA for  $2$  min before SEM observation.

### 2.6. Temperature programmed reduction (TPR)

The temperature programmed reduction (TPR) was conducted to test the oxygen reactivity in OMS-2 catalysts. The TPR experiments were proceeded on OMS-2 catalysts alone without the presence of substrate. The  $5\%$  carbon monoxide (CO) in helium (He) gas was used for the TPR experiments. About  $25$  mg OMS-2 catalyst was placed in a quartz tube with a sintered glass fiber plugged on both ends. The quartz tube was purged with He ( $40$  mL min $^{-1}$ ) at  $120^\circ\text{C}$  to remove adsorbed water. Then the sample was cooled to  $25^\circ\text{C}$  and heated up to  $700^\circ\text{C}$  in a furnace with a programmable controller at a ramp rate of  $10^\circ\text{C min}^{-1}$ . The outlet gas components were monitored with an MKS-UT1 quadrupole mass spectrometer.

## 3. Results and discussion

### 3.1. Internal resistance ( $R_{\text{in}}$ ) and open circuit potentials (OCP) of cathode catalysts

The internal resistances ( $R_{\text{in}}$ ) of GACMFCs with OMS-2 cathodes and Pt cathode are shown in Fig. 2. The  $R_{\text{in}}$  of the Pt cathode was  $17$   $\Omega$ , as well as the Co-OMS-2, Cu-OMS-2, ud-OMS-2 cathodes. However, the  $R_{\text{in}}$  of the Ce-OMS-2 cathode was  $55$   $\Omega$ . The  $R_{\text{in}}$  consists of two parts: the electrolyte ohmic loss caused by the movement of electrons through the electrolyte and the electrode ohmic loss caused by the movement of electrons through the electrode and wires. Because the GACMFCs used in this study had the same configuration (e.g., electrode distance, dimension, and anode materials), the differences of  $R_{\text{in}}$  between GACMFCs may have resulted from the electrical characteristics of different cathodes, especially the conductivity. Regarding the OMS-2 catalysts,

the conductivity included two types: (i) electrical conductivity that was performed under normal (room) temperature; (ii) ionic conductivity that was performed under high temperatures [20]. The EIS results obtained at room temperature showed that the Pt-coated, Co-OMS-2, Cu-OMS-2, and ud-OMS-2 catalysts had good electrical conductivity that led to the low  $R_{\text{in}}$ . However, the electrical conductivity of Ce-OMS-2 was suppressed by the doping of Ce ions, so that Ce-OMS-2 had a higher  $R_{\text{in}}$  than the other four cathodes at room temperature.

The open circuit potential (OCP) was measured to evaluate the electrochemical or biochemical reaction rates on the anode or cathode. The higher OCP values are related to a higher reaction rate [2]. The Co-OMS-2 had a similar OCP ( $147$  mV) as Pt ( $149$  mV), while the other three OMS-2 catalysts had much lower OCPs (Table 1). This indicates that the reaction rates of the Pt and Co-OMS-2 cathodes were theoretically identical. As for the Ce-OMS-2 catalyst, because its electron mobility and catalytic activities are suppressed by the dopants of CeO $_2$ , which is a high temperature ionic conductor [21], its OCP was much lower than other catalysts at room temperature.

### 3.2. Morphology of cathode catalysts

The morphology and compositions of the cathode catalysts analyzed by SEM showed that the application of MnO $_2$  produced structures (like nanowires, Fig. 2A) are different from the Pt-coated cathodes (a flat surface, Fig. 2D). For the OMS-2 catalysts, the nanowire structures increase the surface area and are easier for the organic substrates to be adsorbed on the cathodes. The high surface areas of OMS-2 catalysts could enhance the oxygen absorption and electron acceptance on the catalysts/carbon surface. Three metal ions (Co $^{3+}$ , Cu $^{2+}$ , and Ce $^{4+}$ ) were doped into OMS-2 in order to enhance the catalytic performance in this study. The control of conductivity and redox properties of OMS-2 by doping cations into the framework of OMS-2 could generate higher catalytic activity for ORR. Co $^{3+}$ , and Cu $^{2+}$  ions substitute in the Mn $^{4+}$  positions in the octahedral framework, respectively. Oxygen vacancies created to fulfill an overall charge balance can migrate onto the surfaces of the OMS-2 nanowires and play important roles in catalysis (as shown in Fig. 1). With the nanowire surface properties and the existence of oxygen vacancies, the OMS-2 should substantially increase the oxygen reaction rate and electron acceptance capability. On the other hand, the specific pore and tunnel structures of the OMS-2 catalysts facilitated bacterial growth and adhesion. After  $400$  h of operation, biofilms were clearly observed on the cathodes (Fig. 2B and C).

### 3.3. The performances of cathode catalysts in GACMFCs

The preliminary results from above tests demonstrated that the OMS-2 catalysts had similar electrochemical characteristics as a Pt-coated cathode, indicating that they could be used as the cathodic catalysts in MFCs. In the next step, the OMS-2 catalysts were examined in GACMFCs and compared with Pt in terms of voltage generation and power density. The GACMFCs were operated in a batch mode for  $400$  h with the sodium acetate as the substrate. A refill was done within each cycle before the voltage dropped below  $30$  mV.

Among the four OMS-2 cathode catalysts, the Co-OMS-2 and Cu-OMS-2 catalysts exhibited the best power generation with voltages of  $217$  mV and  $214$  mV, respectively, which were higher than those for the Pt catalyst ( $202$  mV) (Fig. 3). The Ce-OMS-2 and ud-OMS-2 catalysts showed much lower voltage generation, with the voltages of  $142$  mV and  $180$  mV. The low voltage generation of Ce-OMS-2 could be explained by its higher  $R_{\text{in}}$  ( $55$   $\Omega$ , as shown in Table 1). As for the ud-OMS-2 without any metal doping, its catalytic property

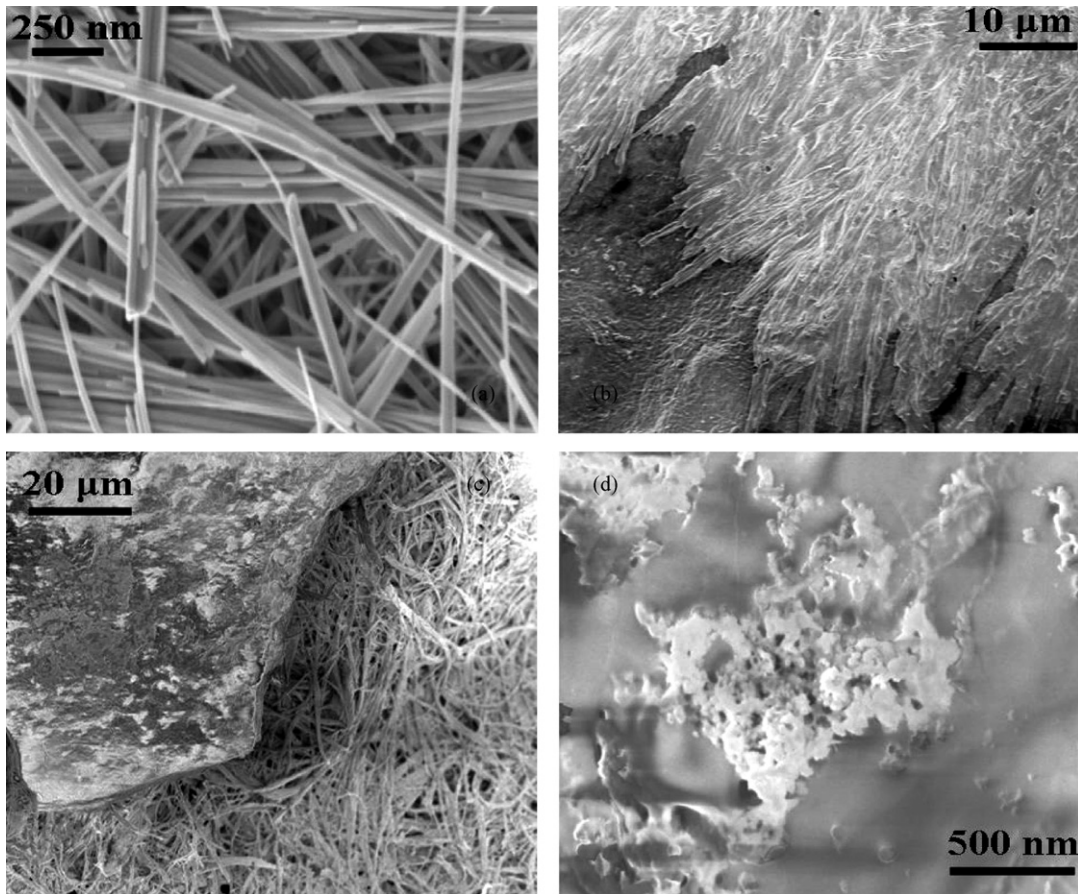


Fig. 2. The SEM images of cathodes. (A) fresh Co-OMS-2 cathode, (B) used Co-OMS-2 cathode, (C) used Cu-OMS-2 cathode with biofilm layer, (D) used Pt cathode.

Table 1

The internal resistances, OCP, maximum power densities, and coulombic efficiencies in GACMFCs with different cathodes.

Cathodes	Internal resistance ( $\Omega$ )	OCP vs. Ag/AgCl (mV)	COD removal efficiency (%)	Maximum power density ( $\text{mW m}^{-2}$ )	Coulombic efficiency (%)
Pt	$18 \pm 1$	149	86.7	198	9.6
Co-OMS-2	$18 \pm 1$	147	99.6	180	8.7
Cu-OMS-2	$18 \pm 1$	116	96.3	165	8.9
Ce-OMS-2	$55 \pm 2$	31	80.0	35	6.6
ud-OMS-2	$18 \pm 1$	82	66.7	86	11.3

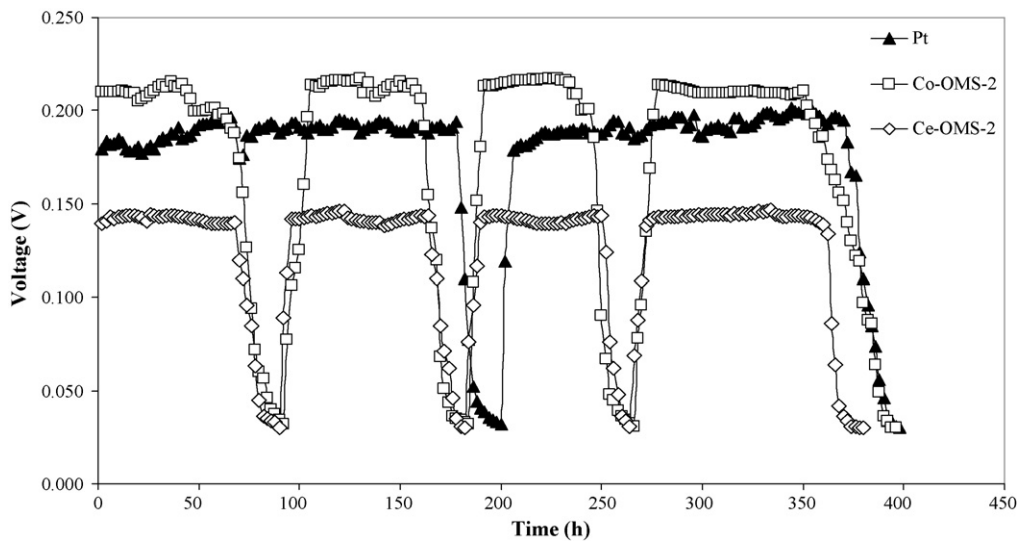


Fig. 3. The voltage generation of the batch-mode GACMFCs with different cathodes.

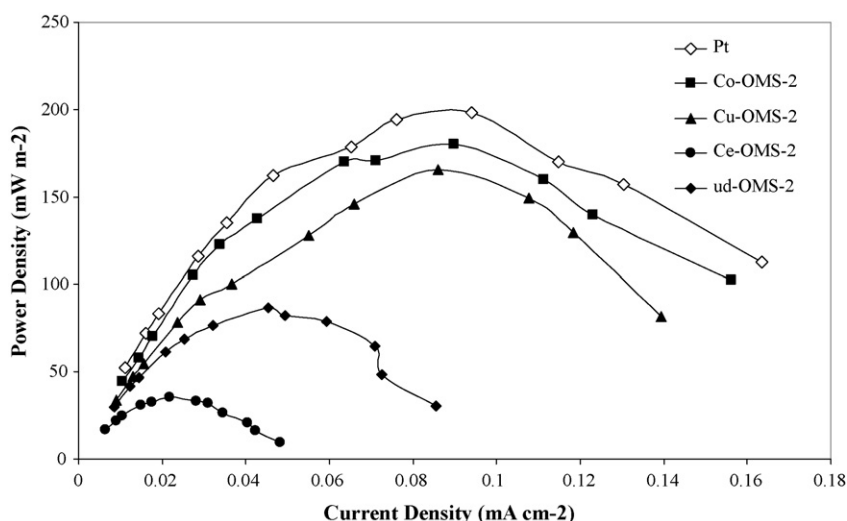


Fig. 4. The power density curves of GACMFCs with different cathodes.

was much lower than those for the Co-OMS-2 and Cu-OMS-2 materials and the power generation was poorer than those for these two catalysts.

The OMS-2 cathodes had twice the reaction rate as the Pt cathodes. The cycle duration of the GACMFCs with a Pt-coated cathode was 202 h, while the cycle duration of the GACMFCs with OMS-2 cathodes was around 90 h (Fig. 3). Because the GACMFCs were operated in a batch mode with the same concentrations of organic substrate, a shorter cycle duration period is related to a faster reaction rate. The GACMFCs with the ud-OMS-2 had a much longer cycle time (108 h, not shown in Fig. 4), which was longer than that for the doped OMS-2 catalysts (90–92 h). This indicated that the metal doping in the cathodes enhanced the oxygen reaction rate (ORR) and the overall biochemical reactions in MFCs. Moreover, the OMS-2 catalysts had higher COD removal efficiencies (85–93%) than the Pt-coated cathode (85%) (Table 1). The ORR of the OMS-2 catalysts was much higher than that for the Pt-coated cathode so that the OMS-2 catalysts could utilize the organic substrate more efficiently, which reveals a great potential of employing OMS-2 catalysts in wastewater treatment plants.

Although the short cycle duration and high COD removal are advantages of the OMS-2 cathode catalysts, they reduced the coulombic efficiencies (CE) correspondingly. The CE values were used to evaluate the conversion of the organic substrates to electricity. Compared to the case with the Pt catalyst, the OMS-2 catalysts had similar voltage generation (Fig. 3) but higher COD removal and shorter cycle duration (Table 1), meaning that the OMS-2 cathode catalysts are effective for COD removal and electricity generation, but not efficient at converting organic substrates to electricity. For instance, the CE value of the Pt-cathode was 9.6%, but the Co-OMS-2 catalyst with the highest voltage generation only had a CE value of 8.7%. The Ce-OMS-2 catalyst with the highest  $R_{in}$  had the lowest CE values of 6.6%. However, the ud-OMS-2 had the highest CE (11.3%), because its cycle time (108 h) was longer than that of the other three OMS-2 catalysts (90–92 h), and has a much lower COD removal efficiency. The CE of ud-OMS-2 was much higher than those for Co-OMS-2 and Cu-OMS-2, even though ud-OMS-2 had a relatively low performance.

The CE values of all the cathodes tested were lower than 12%; the results were consistent with a previous report that high COD loadings led to low CE values [22], which was probably caused by the consumption of organic substrates by bacterial growth rather than by electricity generation. The biofilms were observed on the cathodes (Fig. 2B and 2C), which indicated that the bacterial cells

grew fast at high COD concentration (COD of 3000 mg L<sup>-1</sup> in this study).

Power densities of the OMS-2 catalysts and the Pt catalyst were compared using a polarization curve measurement. The Pt cathode had a higher maximum power density (198 mW m<sup>-2</sup>) than the OMS-2 cathodes (Fig. 4). The Co-OMS-2 and Cu-OMS-2 cathode had power densities of 180 and 165 mW m<sup>-2</sup>, while Ce-OMS-2 and ud-OMS-2 had power densities of 35 and 86 mW m<sup>-2</sup>. The power densities of the OMS-2 cathodes followed the trends of the OCP values (Table 1) and the voltage generation (Fig. 3). That is, the higher OCP values and higher voltage generation were related to the higher power density.

The oxygen reduction activities of the OMS-2 and Pt catalyst were compared using a linear sweep voltammetry (LSV) (Fig. 5). All four OMS-2 catalysts (undoped and doped) produced similar currents over the range of -0.6 V to 0.0 V. When the potential was lower than -1.5 V, the Pt catalyst showed a higher current than the OMS-2 catalysts. However, when the potential was higher than -0.5 V, a higher reduction current was obtained with the OMS-2 catalysts. When the potential was lower than -0.5 V, the order of the reduction current produced by the OMS-2 catalysts was Co-OMS-2 > Cu-OMS-2 > Ce-OMS-2 > ud-OMS-2, which was consistent

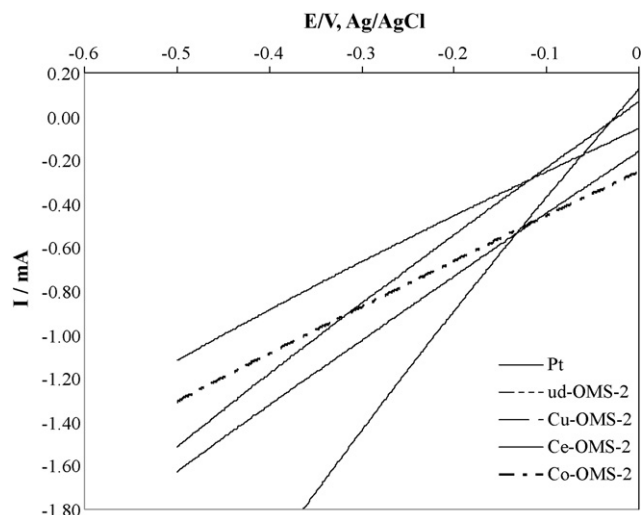
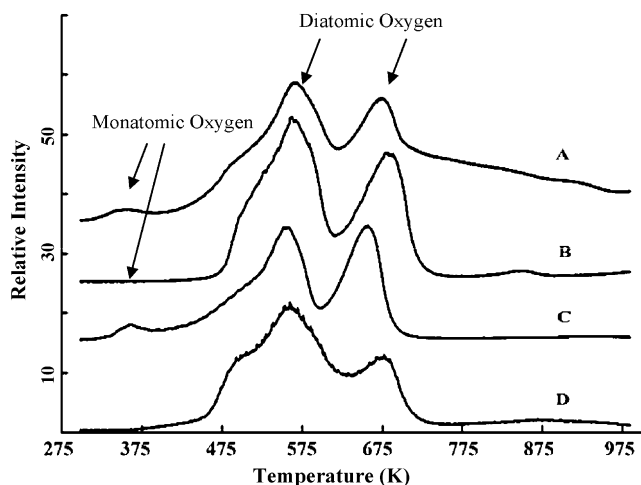


Fig. 5. The linear sweep voltammetry (LSV) for the different cathodes.



**Fig. 6.** The TPR spectra of doped OMS-2 with different metal ions in 5% CO/He. (A) Co-OMS-2, (B) Ce-OMS-2, (C) Cu-OMS-2, (D) ud-OMS-2.

with the OCP results (Table 1). The combined results of the LSV and OCP indicated that the Co-OMS-2 has the highest catalytic activity, and the Cu-OMS-2 is at the second high place.

#### 3.4. Doping effects on the performances of MFCs

Because OMS-2 catalysts involve both the oxygen reduction rate (ORR) and electron acceptance, it is critical to understand the uptake/transition of oxygen species on different OMS-2 catalysts. Temperature programmed reduction (TPR) analysis was employed to determine the amounts of oxygen and the oxygen species to be reduced in cathode reactions for different OMS-2 catalysts. Basically, there were three types of oxygen species in cathode reactions in MFCs: (i) monatomic oxygen, (ii) diatomic oxygen, and (iii) lattice oxygen [23]. In a TPR graph, the response peaks at various temperatures were related to the specific types of oxygen to be reduced at those temperatures. The results showed that all of the OMS-2 catalysts have response peaks related to diatomic oxygen at the temperatures of 575 K and 675 K, which means that all of the OMS-2 catalysts can utilize the diatomic oxygen in the cathode reaction (Fig. 6). However, Co-OMS-2 and Cu-OMS-2 also had peaks assigned to monatomic oxygen at a temperature of 375 K, while ud-OMS-2 and Ce-OMS-2 did not have such peaks. This indicated that Co-OMS-2 and Cu-OMS-2 can utilize more oxygen for the cathode reaction than ud-OMS-2 and Ce-OMS-2. Consequently, these reactive oxygen species in Co-OMS-2 and Cu-OMS-2 catalysts accounted for their higher ORR. This was the reason that the Co-OMS-2 and Cu-OMS-2 catalysts had a higher voltage and power density and a higher COD removal than the Ce-OMS-2 and ud-OMS-2 (as shown in Table 1; Figs. 3 and 4). Hu et al. also conducted thermogravimetric analysis for the adsorption capacity of the OMS-2 catalyst and found that Co-OMS-2 and Cu-OMS-2 had more adsorption and oxidation of substrates than those of the Ce-OMS-2 and ud-OMS-2 [18], which corresponded well with the high COD removal of Co-OMS-2 and Cu-OMS-2 (Table 1).

#### 4. Conclusions

In this study, manganese oxides with the OMS-2 structure were examined as replacements for platinum as the cathode catalyst in

MFCs. The undoped (ud) OMS-2 catalysts and three doped catalysts (Co-OMS-2, Cu-OMS-2, and Ce-OMS-2) were compared in terms of power generation and substrate removal. There were three major conclusions drawn:

First, the OMS-2 catalysts enhanced power generation and substrate degradation efficiency due to their high oxygen reduction rate (ORR). Based on this advantage, the OMS-2 catalysts have a shorter cycle time (90 h) than that of a platinum catalyst (190 h).

Second, compared with a platinum catalyst (cell voltage was 202 mV), the Co-OMS-2 and Cu-OMS-2 cathodic catalysts had higher voltage (217 mV and 214 mV). The OMS-2 doped with metal ions had lower internal resistance, higher power generation, faster reaction rate, and higher substrate removal efficiency than the undoped OMS-2.

Third, since the cost of MnO<sub>2</sub> was only 5% of the platinum cost, the OMS-2 catalysts tested in this study exhibited a great potential to replace platinum as a cathode catalyst for MFC applications in large-scale wastewater treatment plants for efficient contaminant removal and high power generation.

#### Acknowledgements

This project was funded by the Chemical Sciences, Geosciences, and Biosciences Division of the Office of Basic Energy Sciences, and Office of Science, U.S. Department of Energy. Part of the student scholarship was supported by the Multidisciplinary Graduate Research Grant of Center of Environmental Science and Engineering (CESE) and the UConn Provost Outstanding Research Graduate Scholarship. We thank Dr. Frank Galasso for helpful discussions.

#### References

- [1] D. Lovely, Nat. Rev. Microbiol. 4 (2006) 497–508.
- [2] B. Logan, B. Hamelers, R. Rozendal, R. Rozendal, U. Schroder, J. Keller, S. Freguia, P. Aelterman, W. Verstraete, K. Rabaey, Environ. Sci. Technol. 40 (2006) 5181–5192.
- [3] Y. Zuo, S. Cheng, B. Logan, Environ. Sci. Technol. 42 (2008) 6967–6972.
- [4] P. Aelterman, M. Verschele, M. Marzorati, N. Boon, W. Verstraete, Bioresour. Technol. 99 (2008) 8895–8902.
- [5] J. Jang, T. Pham, I. Chang, K. Kang, H. Moon, Process Biochem. 39 (2004) 1007–1012.
- [6] T. Pham, J. Jang, I. Chang, B. Kim, J. Microbiol. Biotechnol. 14 (2004) 324–334.
- [7] H. Liu, B. Logan, Environ. Sci. Technol. 38 (2004) 4040–4046.
- [8] A. Heijne, H.M. Hamelers, C.N. Buisman, Environ. Sci. Technol. 41 (2007) 4130–4134.
- [9] S. Cheng, H. Liu, B. Logan, Environ. Sci. Technol. 40 (2006) 364–369.
- [10] J. Rebello, P. Samant, J. Figueiredo, J. Fernandes, J. Power Sources 153 (2006) 36–40.
- [11] R.X. Feng, H. Dong, Y.D. Wang, X.P. Ai, Y.L. Cao, H.X. Yang, Electrochem. Commun. 7 (2005) 449–452.
- [12] L. Zhang, C. Liu, L. Zhuang, W. Li, S. Zhou, J. Zhang, Biosens. Bioelectron. 24 (2009) 2825–2829.
- [13] I. Roche, K. Katuri, K. Scott, J. Appl. Electrochem. (2009) doi:10.1007/s10800-009-9957-4.
- [14] S. Suib, J. Mater. Chem. 18 (2008) 1623–1631.
- [15] S. Suib, Acc. Chem. Res. 41 (2008) 479–488.
- [16] Y. Son, V. Makwana, A. Howell, S. Suib, Angew. Chem. Int. Ed. 40 (2001) 4280–4283.
- [17] J. Yuan, K. Laubernds, J. Villegas, S. Gomez, S. Suib, Adv. Mater. 16 (2004) 1729–1732.
- [18] B. Hu, C. Chen, L. Jin, S. Frueh, S. Suib, Proc. 238th ACS National Meeting, Washington, DC, August 16–20, 2009.
- [19] D. Jiang, B. Li, Biochem. Eng. J. 47 (2009) 31–37.
- [20] L. Chen, C.L. Chen, D.X. Huang, Y. Lin, X. Chen, A.J. Jacobson, Solid State Ionics 175 (2004) 103–106.
- [21] C. Xia, Y. Li, Y. Tian, Q. Liu, Y. Zhao, L. Jia, Y. Li, J. Power Sources 188 (2009) 156–162.
- [22] H. Liu, S. Cheng, B. Logan, Environ. Sci. Technol. 39 (2005) 5488–5493.
- [23] Y. Yin, W. Xu, Y. Shen, S. Suib, C. O'Young, Chem. Mater. 6 (1994) 1803–1808.